Subspace Based Identification of Power Transformer Models from Frequency Response Data

Hüseyin Akçay, § Syed M. Islam, † and Brett Ninness ‡

Abstract— **A recent frequency-domain, subspace-based algorithm is used in the identification of two power transformers. The results indicate that the subspace-based identification algorithms can be used without modification even when the dynamic range of frequency response data is large.**

Key words: Identification, frequency response data, power transformer, subspace-based algorithm.

I. Introduction

Frequency response methods are often used in practice to obtain a nonparametric model of a linear system. This identification may be performed without significant *a priori* knowledge of the plant. Further, if the excitation of the system is well-designed, *e.g.,* periodic input or stepped sine, each transfer function measurement, compiled from a large number of time-domain measurements, is of high quality. Also, data obtained from different experiments can easily be combined in the frequency domain.

The problem of fitting a real-rational model to a given frequency response data set has been addressed by many authors [14], [13], [15], [8]. In the classical approach, a system is modeled as a fraction of two real coefficient polynomials and a nonlinear least-squares fit to data is sought. This nonlinear parametric optimization problem is solved by iterative, numerical search. Recently however, some noniterative, frequency-domain, subspace-based identification algorithms which deliver state-space models without any parametric optimization have appeared in the literature [7], [11]. The subspace-based algorithms have been successfuly used in the identification of high-order flexible structures [7], [11].

In this paper, the objective is to illustrate the properties of the recent frequency-domain, subspace-based identification algorithms in a case study where the dynamic range of frequency response data is large. A major motivation for the case study in the present work is the challenge posed by power transformers. High frequency modelling is essential in the design of power transformers to study impulse voltage and switching surge distribution, winding integrity and insulation diagnosis and most often high fidelity models in a bandwidth up to 10 MHz are required for condition monitoring purposes. The study of a high frequency part of the spectra is necessary due to the resulting stray capacitances shunting the series inductances and dominating the response. Accurate parameter identification of transformers may lead to economical design of transformer insulation against failure due to ferro-resonance and through fault generated stresses.

Dick and Even [3] proposed the frequency response analysis method for the detection of winding movement in large power transformers. In [3], as a practical maintanence tool, certain advantages of frequency domain approach over the low voltage impulse method [6] are reported. The research using the transfer function method to date has been mainly limited to interpreting faults by detecting changes in successive frequency response tests. However, this approach fell short in explaining the changes in relation to a suitably developed mathematical model. In [5] and other works, transformer frequency response is divided into low, medium, and high frequency ranges and a second order model fit to data is sought. In [5], the nonlinear least-squares method is applied to obtain an appropriate transfer function to model the frequency response of a particular transformer from 50 Hz to 1MHz. The models obtained by this approach poorly fit data and in particular are not capable of modelling high frequency dynamics of a transformer.

The current paper focuses on mathematical models of transformers rather than their equivalent circuits. Our view is that once an accurate analytic model of the transformer under consideration is available, it is possible to derive a transformer equivalent circuit by a suitable transformation if necessary. This subject is currently under investigation. As well, our case study indicates that transformer dynamics varies from one transformer to another which makes it difficult to derive a transformer equivalent circuit valid for all range of power transformers. Nevertheless, a mathematical model adequately describes a transformer for the purposes of studying its time domain response and monitoring its condition in service.

In § 2, we describe the experimental data to which the subspace-based identification algorithm will be applied. In § 3, we outline the subspace algorithm used in this paper. In § 4, we present our identification results applied to two three winding transformers. § 5 concludes the paper.

This work was supported by TÜBİTAK, the Centre for Integrated Dynamics and Control (CIDAC), and Australian Research Council, which is gratefully acknowledged.

§ Dept. of Electrical and Computer Engineering, University of Newcastle, Callaghan, NSW 2308, Australia. Fax: +(61) 49 216993. e-mail: akcay@ee.newcastle.edu.au. On leave from TÜBİTAK, Marmara Research Center, Division of Mathematics, P.0. Box 21, Gebze–KOCAELI, Turkey. Corresponding author.

† Dept. of Electrical and Computer Engineering. Curtin University of Technology, GPO Box U 1987, Perth, WA 6001, Australia.

‡ Dept. of Electrical and Computer Engineering and CIDAC, University of Newcastle, Callaghan, NSW 2308, Australia.

II. Experimental Data

In this section, we describe the experimental data sets. The two data sets were obtained from the Advanced Technology Center of Pacific Power International, Newcastle, Australia from the tests conducted on power transformers in New South Wales. The data sets were obtained from two identical transformers. Each transformer is a 132/66/11kV, 30MVA unit with a YyN0d1 vector grouping. Both transformers were placed in-service in the mid-1960's. At present, one of the transformers which we call for brevity A1 is in service while the other unit called T1 failed in-service in January 1996.

A. Test and Measurement Process

The transformers were prepared for test by being removed from service and electrically isolated from the transmission system. For those windings which were delta connected, the delta points were dis-jointed. For star windings, the neutral points were earthed, and the tests were conducted on one phase pair at a time. Transformer tap positions were noted. The instruments used to conduct the tests were an arbitrary wave/function generator, a cathode ray oscillope (CRO), and a PC with a portable general purpose interface bus (GPIB) card. Essentially, the test methodology consisted of using the arbitrary wave generator to inject a signal into one of the phase windings, then using the CRO to measure this input voltage, its frequency, the corresponding output voltage and the time lag between the output and input signals. The information measured by the CRO was transferred via a program (with the use of the GPIB card) to the computer. The program obtained the maximum and minumum values of each waveform from the oscilloscope, then calculated the mean and amplitude of the waveform. Next the phase shift for each sine wave was computed from the time delay between the input and output signals using the mean and amplitude information. The tests were conducted over a wide range of frequencies from 50Hz to 200 kHz. We refer the interested reader to [2] for more details on the experimental procedure.

B. Transformers A1 and T1 Data

Transformers A1 and T1 are both 3-winding transformers. The frequency response magnitudes of Phase a–c plotted in Fig. 1–2 were obtained by injecting a low voltage amplitude into the TV winding of the transformers over a frequency range of 50Hz to 200kHz and measuring the output voltage at the LV winding. The numbers of frequency points in Fig. 1 are respectively, 125, 123, and 121. Notice that all the three responses are almost identical. For this reason, we will work only with Phase a frequency response. In Fig. 2, Phase a–c frequency response magnitudes of T1 are plotted. The numbers of frequency points in Fig. 2 are 123, 137, and 125 respectively for Phase a, b, and c. Phase a response of Transformer T1 has changed dramatically after the failure, *i.e.,* through fault generated large electrical stress, which is observable from the magnitude plot, whereas Phase b–c responses of T1 do not significantly differ from those of A1.

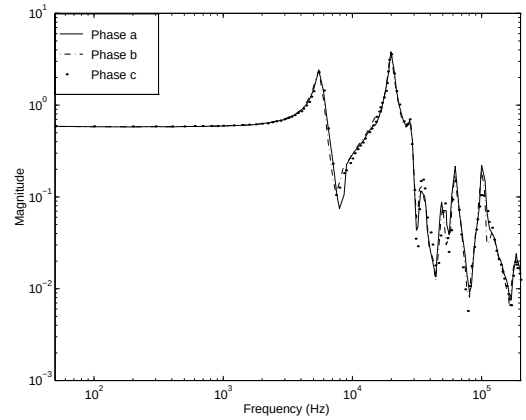

Fig. 1. Phase a–c frequency response magnitudes of Transformer A1.

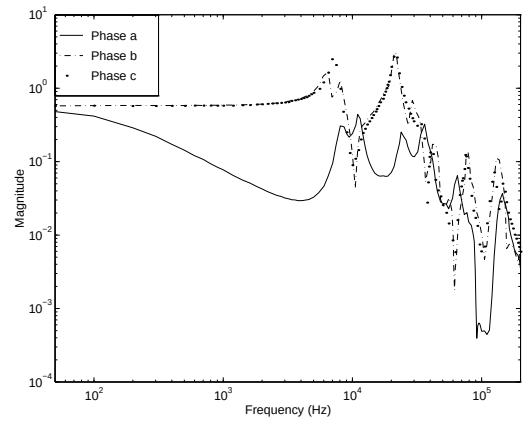

Fig. 2. Phase a–c frequency response magnitudes of Transformer T1.

III. Subspace-Based Identification in Frequency Domain

In this section, we introduce the subspace based identification algorithm used in this paper. This algorithm was presented in [11] and its theoretical properties as well as its applications to identification of lightly damped flexible structures were reported in [11], [12]. See [11] for detailed motivation of this algorithm. The focus of the current paper is its application to power transformer identification.

Suppose that the "true" unknown system to be identified is a stable, multi-input/multi-output, linear time-invariant, continuous-time system with input-output properties charecterized by the impulse response function $g(t)$ through the equation

$$y(t) = \int_0^\infty g(s)u(t-s)\ dt \tag{1}$$

where $y(t) \in \mathbf{R^p}$, $u(t) \in \mathbf{R^m}$, and $g(t) \in \mathbf{R^{p\times m}}$. We also assume that the system is of finite order n and thus can be described by a state-space model

$$\begin{aligned} \dot{x}(t) &= Ax(t) + Bu(t) \\ y(t) &= Cx(t) + Du(t) \end{aligned} \tag{2}$$

where $x(t) \in \mathbf{R^n}$. The state-space model (2) has the impulse response

$$g(t) = D\,\delta(t) + Ce^{jAt}B$$

where δ is Dirac's delta function. The frequency response of (1) is calculated as

$$G(j\omega) = \int_0^\infty g(t)e^{-j\omega t}\,dt, \quad -\infty \le \omega \le \infty$$

which for the state-space model (2) can be written as

$$G(j\omega) = C\,(j\omega I_n - A)^{-1}\,B + D. \tag{3}$$

In (3), $j = \sqrt{-1}$ is the imaginary unit and I_n denotes the $n \times n$ identity matrix.

Suppose that we are given N noise-corrupted samples of the frequency response function

$$G_k = G(j\omega_k) + n_k, \quad k = 1, \cdots, N.$$

The objective is to devise an identification algorithm which maps data G_k into a finite-dimensional transfer function $\widehat{G}$. In estimating the transfer function, we will use the following algorithm.

Algorithm:

1. Bilinearly transform the given data G_k, ω_k as

$$\begin{aligned} G_k^d &= G_k, \quad k = 1, \cdots, N \\ \theta_k &= 2\,\mathrm{atan}\left(f^{-1}\omega_k\right), \quad k = 1, \cdots, N \end{aligned}$$

   where f is twice the bandwidth of the system (in Hertz).

2. Extend the discrete-time transfer function samples G_k^d to the full unit circle

$$G_{N+k}^d = [G_{N-k+1}^d]^*, \quad k = 1, \cdots, N$$

   where $(\cdot)^*$ denotes complex conjugate.

3. Form the matrices $\mathbf{G}$ and W

$$\mathbf{G} = \frac{1}{\sqrt{M}} \begin{bmatrix} G_1^d & \cdots & G_M^d \\ e^{j\theta_1}G_1^d & \cdots & e^{j\theta_M}G_M^d \\ \vdots & \ddots & \vdots \\ e^{j(q-1)\theta_1}G_1^d & \cdots & e^{j(q-1)\theta_M}G_M^d \end{bmatrix}$$

$$\mathbf{W} = \frac{1}{\sqrt{M}} \begin{bmatrix} I_m & \cdots & I_m \\ e^{j\theta_1}I_m & \cdots & e^{j\theta_M}I_m \\ \vdots & \ddots & \vdots \\ e^{j(q-1)\theta_1}I_m & \cdots & e^{j(q-1)\theta_M}I_m \end{bmatrix}$$

   where $M = 2N$.

4. Calculate the QR-factorization

$$\begin{bmatrix} \mathrm{Re}\mathbf{W} & \mathrm{Im}\mathbf{W} \\ \mathrm{Re}\mathbf{G} & \mathrm{Im}\mathbf{G} \end{bmatrix} = \begin{bmatrix} \mathbf{R}_{11} & 0 \\ \mathbf{R}_{21} & \mathbf{R}_{22} \end{bmatrix} \begin{bmatrix} \mathbf{Q}_1^T \\ \mathbf{Q}_2^T \end{bmatrix}.$$

5. Calculate the SVD

$$\mathbf{R}_{22} = \hat{U}\,\hat{\Sigma}\,\hat{V}^T.$$

6. Determine the system order n by inspecting the singular values and partition the SVD such that $\hat{\Sigma}_s$ contains the n largest singular values

$$\mathbf{R}_{22} = \begin{bmatrix} \hat{U}_s & \hat{U}_o \end{bmatrix} \begin{bmatrix} \hat{\Sigma}_s & 0 \\ 0 & \hat{\Sigma}_o \end{bmatrix} \begin{bmatrix} \hat{V}_s^T \\ \hat{V}_o^T \end{bmatrix}.$$

7. Determine the discrete-time system matrices A^d and C^d as

$$\begin{aligned} A^d &= \left(J_1\hat{U}_s\right)^\dagger J_2\hat{U}_s \\ C^d &= J_3\hat{U}_s \end{aligned}$$

   where J_i are defined by

$$\begin{aligned} J_1 &= \begin{bmatrix} I_{(q-1)p} & 0_{(q-1)p\times p} \end{bmatrix} \\ J_2 &= \begin{bmatrix} 0_{(q-1)p\times p} & I_{(q-1)p} \end{bmatrix} \\ J_3 &= \begin{bmatrix} I_p & 0_{p\times(q-1)p} \end{bmatrix} \end{aligned}$$

   and $0_{i\times j}$ denotes the $i \times j$ zero matrix and $X^\dagger = (X^TX)^{-1}X^T$ the Moore-Penrose pseudo inverse of the full column rank matrix X.

8. If A^d has unstable eigenvalues, add the following stability ensuring projection step:
   - Transform A^d to the complex Schur form with the eigenvalues on the diagonal.
   - Project any diagonal elements (eigenvalues) satisfying $1 < |\lambda_i| \le 2$, into the unit disc by $\lambda_i' \triangleq \lambda_i(\frac{2}{|\lambda_i|} - 1)$. Eigenvalues with magnitude $|\lambda_i| > 2$ are set to zero. Eigenvalues on the unit circle can be moved into the unit disc by changing the magnitude of the eigenvalue to $1 - \epsilon$ for some small positive ϵ, *i.e.*, $\lambda_i' \triangleq \lambda_i(1-\epsilon)$.
   - Finally transform A^d back to its original form.

9. Solve the following least-squares problem to determine B^d and D^d

$$\sum_{k=1}^{M} \left\| G_k^d - D - C^d\left(e^{j\theta_k}I_n - A^d\right)^{-1}B \right\|_F^2$$

   where $\|X\|_F = \sqrt{\sum_{k,s}|x_{ks}^2|}$ denotes the Frobenius norm.

10. The estimated continuous-time transfer function is defined as

$$\widehat{G}(s) = \widehat{D} + \widehat{C}\left(sI_n - \widehat{A}\right)^{-1}\widehat{B}$$

   where the continuous-time state-space parameters $(\widehat{A}, \widehat{B}, \widehat{C}, \widehat{D})$ are obtained from the discrete-time state-space parameters (A^d, B^d, C^d, D^d) as

$$\begin{aligned} \widehat{A} &= f\,\left(I_n + A^d\right)^{-1}\left(A^d - I_n\right) \\ \widehat{B} &= \sqrt{2f}\,\left(I_n + A^d\right)^{-1}B^d \\ \widehat{C} &= \sqrt{2f}\,C^d\left(I_n + A^d\right)^{-1} \\ \widehat{D} &= D^d - C^d\left(I_n + A^d\right)^{-1}B^d. \end{aligned}$$

The algorithm outlined above is noniterative and does not require the frequencies be uniformly spaced. In Step 1, the bilinear transformation

$$s = f\,\frac{z-1}{z+1} = \psi(z)$$

is applied to convert the problem to an equivalent discrete-time identification problem and in Step 10, the estimated continuous-time transfer function is obtained from the estimated discrete-time transfer function by back transformation:

$$\widehat{G}(s) = C^d\left(\psi^{-1}(z)\,I_n - A^d\right)^{-1} B^d + D^d.$$

The transformation ψ and its inverse ψ^{-1} preserve maximums of transfer function magnitudes. Step 2 ensures the estimated system will have real valued parameters. In Step 3–7, the computation of A^d and B^d is based on the shift-invariance structure of extended observability matrix.

Before we move to the next section, we make the following observations on the choice of parameters q, n and ϵ:

- To obtain best accuracy, $q \leq M$ should be chosen as large as possible.
- The best model order in Step 6 yielding the smallest error tends to be high. We recommend Step 5 be repeated until a satisfactory model order is obtained comprimising both accuracy and model complexity. An alternative strategy is to successively reduce a high order $\hat{G}$ by the balanced truncation method.
- In Step 8, we suggest ϵ be chosen to satisfy $\epsilon \leq \min_{1<\lambda_i\leq 2}(|\lambda_i| - 1)$. The reason for this choice is that when G is lightly damped and especially has a large bandwidth, the discrete-time identified poles in Step 6 tend to cluster around the unit circle and a large value for ϵ may yield low accuracy. Most often, in particular when signal-to-noise ratio is high and model order is not taken very large, the projection step is not needed.
- An alternative stability ensuring method was proposed in [9] by the following procedure

$$A^d = \hat{U}_s^{\dagger}\begin{bmatrix} J_2^q \hat{U}_s \\ 0_{p\times n} \end{bmatrix}.$$

  This step should be applied whenever the original A^d is unstable.

IV. Experimental Identification Results

In this section, we will discuss the results obtained from application of the identification algorithm described in § 3. We take $f = \max_k \omega_k/\pi$ which coincides with twice the Nyquist frequency when G is bandlimited and frequencies are uniformly spaced. For greater flexibility, its value can be adjusted as well.

A. Quality Measures

The quality of estimated models will be assessed by two measures based on the fit between the data and the model. The maximum error

$$\|\widehat{G} - G\|_{m,\infty} = \max_k |\widehat{G}(j\omega_k) - G_k| \tag{4}$$

and the root-mean-square error (rms)

$$\|\widehat{G} - G\|_{m,2} = \sqrt{\frac{1}{N}\sum_{k=1}^{N} |\widehat{G}(j\omega_k) - G_k|^2}. \tag{5}$$

B. Model Order Determination

We start by trying to determine an appropriate model order by the cross-validation technique [17]. We divide the data set into two disjoint sets, the estimation data and validation data. The division is made such that every odd numbered frequency response sample is put in the estimation set and every other in the validation set. Models of different orders are determined from the estimation data, and then model order is determined at the frequency points of the validation data. The underlying assumption is that if one begins with a low model order, the error on validation data will decrease as the model order increases until an appropriate model order is found.

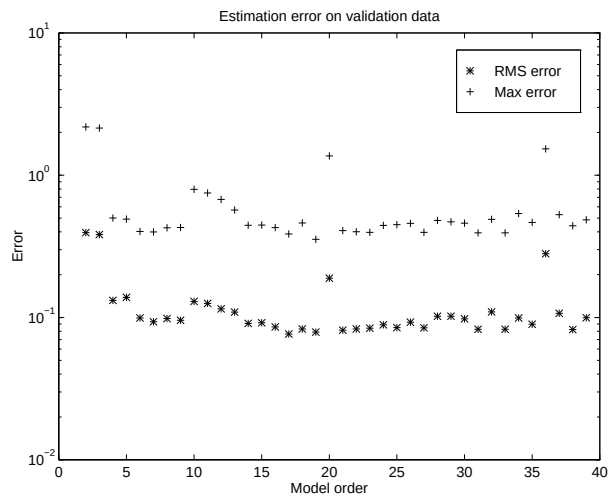

Fig. 3. Model errors (4)–(5) for Phase a response of Transformer A1 calculated on independent validation data using subspace-based algorithm.

Applying subspace algorithm to Phase a frequency response of A1, a sequence of models of order 2–39 are estimated for $q = 40$ and $N = 62$. The frequency response of each estimated model is calculated at the frequencies of the validation data and the rms and max errors (4)–(5) are determined using the 62 point validation data set. The results are shown in Fig. 3. From the graph, it is hard to judge a correct model order. At best, some isolated cases are ruled out. This could be attributed to the insufficient number of data available for the estimation. The calculated eight singular values in Step 6 of the algorithm are 1.9611, 1.8849, 1.2063, 0.9951, 0.2578, 0.2419, 0.0903, 0.0866, which suggest that model order must be at least 6. In Fig. 4–5, measured and estimated 6th and 31st order model frequency responses are plotted. In the estimation of

model orders, the complete data record was used. In particular, Fig. 5 shows the excellent fit obtained by the subspace method. Notice that model responses are almost identical up to 30 kHz. In Fig. 6, the frequency responses of 17th and 6th order identified models and the model obtained by truncating balanced realization of the former are plotted. Fig. 6 supports our view that low order models obtained either directly by the subspace algoritm or indirectly truncating balanced realization of a high order model identified by the subspace algorithm have the same accuracy.

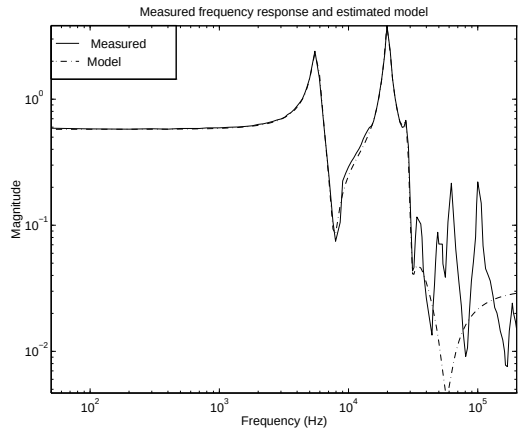

Fig. 4. Measured and estimated 6th order model Phase a frequency response magnitudes of Transformer A1 using subspace based algorithm.

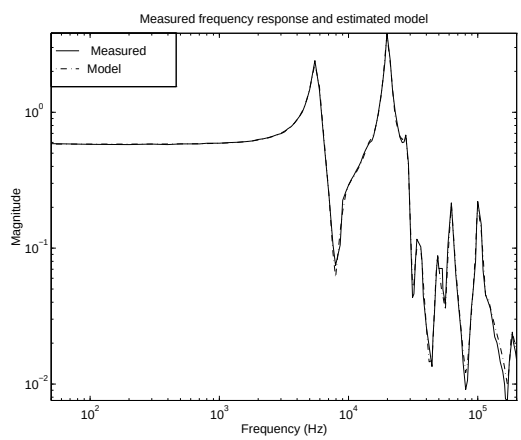

Fig. 5. Measured and estimated 31st order model Phase a frequency response magnitudes of Transformer A1 using subspace based algorithm.

Next we apply the subspace algorithm to Phase a frequency response of Transformer T1. A sequence of models of order 1–20 are estimated for $q = 40$ and $N = 61$. The model validation results are plotted in Fig. 7. From the figure, it is seen that both the rms and maximum errors are minimized for the 17th order model. Indeed, Fig. 8 shows the excellent fit obtained for the 17th order model. The high frequency fit to data can even be further improved by using higher order models as shown in Fig. 9 for the

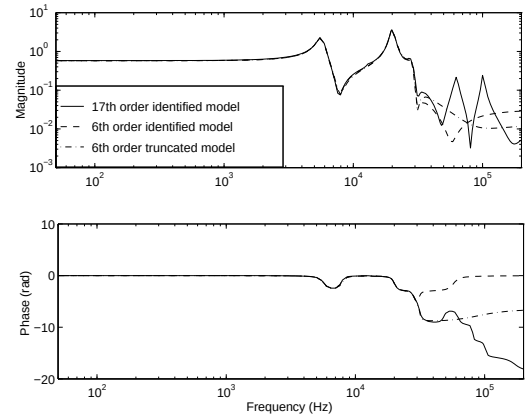

Fig. 6. Estimated and reduced model Phase a frequency responses of Transformer A1. 17th and 6th order models are estimated using subspace based algorithm and reduced model is extracted from the balanced realization of 17th order model.

31st order identified model. It is evident from Phase c frequency response magnitude plotted in Fig. 2 that a 6th order model is not suitable to capture the dynamics of a failed-in three winding transformer. Transformer failures are usually accompanied by the generation of new modes and the disappearance of old modes as shown in Fig. 8. Existing mode shapes and natural frequencies are also subject to dramatic changes. This variation of model structure makes it difficult to correlate winding deformations to the elements of transformer equivalent circuit.

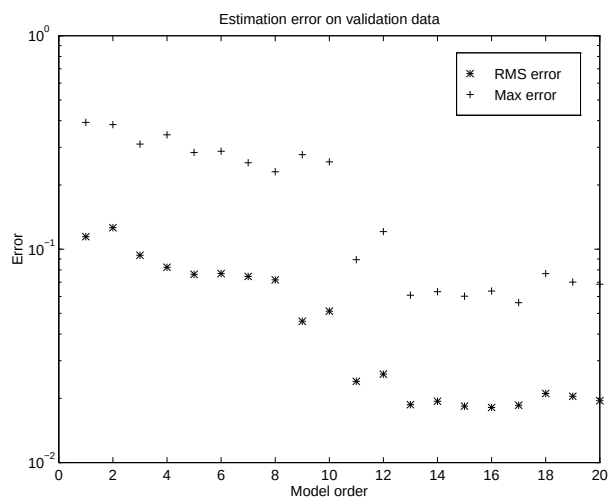

Fig. 7. Model errors (4)–(5) for Phase a of Transformer T1 calculated on independent validation data using subspace-based algorithm.

We have also tried two nonlinear least-squares (NLS) algorithms as implemented by **invfreqs** and **invfreqz** commands in MATLAB on Phase a frequency responses of Transformers A1 and T1. We observed that the identification errors (4)-(5) fluctuated with model order in contrary to the pattern seen in Fig. 7. In passing, there is a parametric identification algorithm in [16] developed for systems with a large dynamic range, which might be applicable to the transformer identification problem considered in this paper.

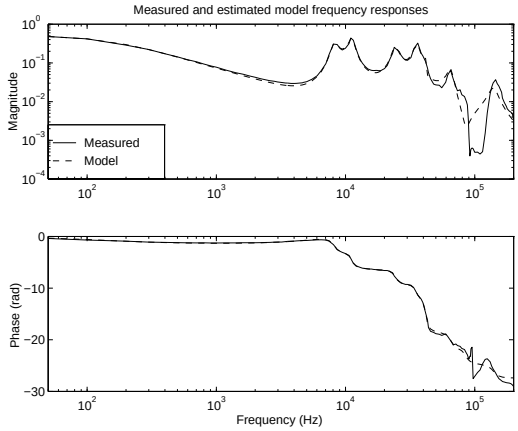

Fig. 8. Measured and estimated 17th order model Phase a frequency responses of Transformer T1 using subspace based algorithm.

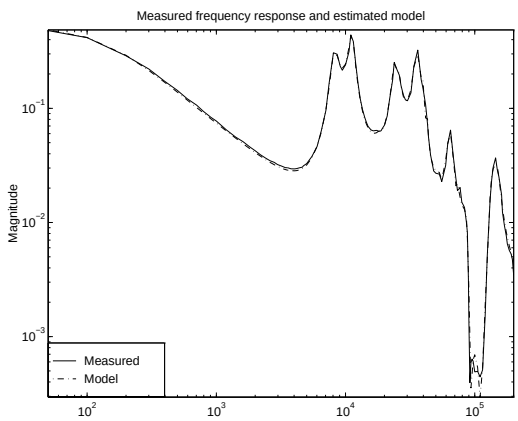

Fig. 9. Measured and estimated 31st order model Phase a frequency response magnitudes for Transformer T1 using subspace based algorithm.

V. Conclusions

In this paper, we applied a recently developed subspace-based identification algorithm to obtain mathematical models of power transformers from frequency response data. Models delivered by the subspace-based identification algorithm can be refined further by parametric optimization techniques such as the maximum likelihood search. Mathematical models are sufficient for a study of transient response of transformer and monitoring its condition in service. The proposed model development may be viewed as the first step towards deriving a transformer equivalent circuit. Our view is that once an analytical transformer model is available, it is rather straightforward to derive the parameters of an equivalent circuit to match the frequency response of the model. This approach is currently under investigation. The traditional second or third order transformer equivalent circuits [3], [1], [10], [4], [5] do not capture the dynamics of realistic power transformers. The combination of finite-element methods with the subspace-based identification algorithms may produce accurate transformer equivalent circuits from frequency response data.

References

[1] J. Bak-Jensen, B. Bak-Jensen, S. D. Mikkelsen, and C. G. Jensen, "Parametric identification in potential transformer modelling," *IEEE Trans. Power Delivery,* vol. 7, pp. 70–76, 1992.

[2] K. Coates, "Condition monitoring of power transformers using transfer functions," *Senior Project*, Dept. Elec. Comp. Eng., the University of Newcastle, Australia, 1996.

[3] E. P. Dick and C. C. Even, "Transformer diagnostic testing by frequency analysis," *IEEE Trans. Power Apparatus Syst.*, vol. PAS-97, pp. 2144–2153, 1978.

[4] D. A. Douglas, "Potential transformer accuracy at 60 Hz voltages above and below rating and at frequencies above 60 Hz," *IEEE Trans. Power Apparatus Syst.,* vol. PAS-100, pp. 1370–1375, 1981.

[5] S. M. Islam, K. M. Coates, and G. Ledwich, "Identification of high frequency transformer equivalent circuit using MATLAB from frequency domain data," in *IEEE Industry. Appl. Soc.,* Annual Meeting, New Orleans, Lousiana, 1997.

[6] W. Lech and L. Tyminski, "Detecting transformer winding damage-the low voltage impulse method," *Electrical Review,* vol. 179:21, pp. 768–772, 1966, (ERA Translation).

[7] K. Liu, R. N. Jacques, and D. W. Miller, "Frequency domain system identification by observability range space extraction, " *ASME Trans. J. Dynamic Syst. Measurement Contr.,* vol. 118, pp. 211–220.

[8] L. Ljung, "Some results on identifying linear systems using frequency domain data, in *Proc. 32rd IEEE Conf. Dec. Contr.,* San Antonio, TX, Dec. 1993, pp. 3534–3538.

[9] J. M. Maciejowski, "Guaranteed stability with subspace Methods," *Syst. Contr. Lett.*, vol. 26, pp. 153–156, 1995.

[10] R. Malewski and B. Poulin, "Impulse testing of power transformers using the transfer function method," *IEEE Trans. Power Delivery*, vol. 3, pp. 476–489, 1988.

[11] T. McKelvey, H. Akçay, and L. Ljung, "Subspace-based multivariable system identification from frequency response data," *IEEE Trans. Automat. Contr.,* vol. 41, pp. 960–979, 1996.

[12] T. McKelvey, H. Akçay, and L. Ljung, "Subspace-based identification of infinite-dimensional multivariable systems from frequency response data," *Automatica,* vol. 32, pp. 885–902, 1996.

[13] R. Pintelon, P. Guillaume, Y. Rolain, and H. Van Hamme, "Parametric identification of transfer functions in the frequency domain–A survey," *IEEE Trans. Automat. Contr.,* vol. AC-39, pp. 2245–2260, 1994.

[14] C. K. Sanathanan and J. Koerner, "Transfer function synthesis as a ratio of two complex polynomials," *IEEE Trans. Automat. Contr.,* vol. AC-8, pp. 56–58, 1963.

[15] J. Schoukens and R. Pintelon, *Identification of linear systems: A Practical Guideline to Accurate Modeling.* London: Pergamon, 1991.

[16] M. D. Sidman, F. E. DeAngelis, and G. C. Verghese, "Parametric system identification on logarithmic frequency response data," *IEEE Trans. Automat. Contr.,* vol. AC-36, pp. 1065–1070, 1991.

[17] P. Stoica, P. Eykhoff, P. Janssen, and T. Soderstrom, "Model structure selection by cross validation," *Int. J. Contr.,* vol. 43, pp. 1841–1878, 1986.